Supplementary Material for:
Effectively Distinguishing Blast and Earthquake Sources in Eastern Canada

Justin Chien[1,*], Yajing Liu[1]

[1]Department of Earth and Planetary Sciences, McGill University, Montréal, QC, Canada

[*]Corresponding author: shihhan.chien@mail.mcgill.ca

Introduction

In this Supporting Information, we briefly describe the catalog-enhancement procedure in Text S1, and we provide an example in Text S2 showing how an additional feature can be incorporated into the final fully connected layer of a pre-trained convolutional neural network. The supporting figures mainly accompany the main manuscript to improve readability and to illustrate representative waveform examples. We also provide a supplementary spreadsheet containing the complete model evaluation results. Specifically, the sheets baseline_results_with_nohour and baseline_results_with_hour summarize the baseline model comparisons without and with the origin-hour feature, respectively. The sheet with_hour_optimized_cost_test presents the further optimization results for the three best-performing models selected from the baseline comparison, and top_model_random_seed_test reports the five-random-seed experiments used to identify the final model. In addition, event_level_classification_10se summarizes event-level classification performance after applying the weighting procedure described in the main text for different minimum-station conditions. Finally, blast_subsample_posweight_test reports sensitivity tests examining how different retained fractions of blast events influence model performance. The final table compares the machine-learning-enhanced catalog with the Canadian National

Earthquake Database (NEDB) in the Western Québec Seismic Zone, in order to demonstrate the effectiveness of the newly developed discriminator.

Text S1. We first applied the ML-based phase picker EqTransformer (Mousavi et al., 2020), using a conservative model tuned to minimize false positives. Given the high occurrence of overlapping blasts in this region, we set the P/S phase threshold to 0.1and the earthquake detection threshold to 0.3. We then employed PyOcto (Münchmeyer, 2023) for phase association, adopting the Eastern Canada 1D velocity model from Kao et al. (2012). Our criteria required a minimum of three stations each detecting both P and S phases, and a total of at least eight phase picks. Finally, we used NonLinLoc (Lomax et al., 2000) to estimate initial event locations and calculate local magnitude with Nuttli magnitude relationship (Nuttli, 1973).

Text S2. To incorporate origin-time information into the CNN classifier, we modified the standard ResNet architecture by appending an auxiliary hour-feature branch to the image backbone. First, the final fully connected classification layer of the pretrained ResNet18 or ResNet50 model was removed, and the remaining convolutional layers were used as a feature extractor for the three-channel spectrogram input. This backbone produces a compact image-feature vector of dimension 512 for ResNet18 or 2048 for ResNet50 after global average pooling.

In parallel, the event-origin-time feature was provided as an additional numerical input. This hour feature was passed through a small fully connected layer that maps the input

hour representation to a 16-dimensional latent feature vector, followed by a ReLU activation. Dropout regularization was applied separately to the image-feature branch and the hour-feature branch. The extracted spectrogram features and transformed hour features were then concatenated and passed through a final fully connected layer to produce a single output logit for binary classification. A further dropout layer was applied after concatenation before the final output layer. In this way, the network jointly learns discriminative information from both the spectrogram morphology and the event origin-time feature, allowing temporal information to contribute directly to the final earthquake-versus-blast decision.

This design allows the model to integrate both spectrogram-derived information and temporal context into a unified classification framework. Please refer to (Chien, 2025) for more detail.

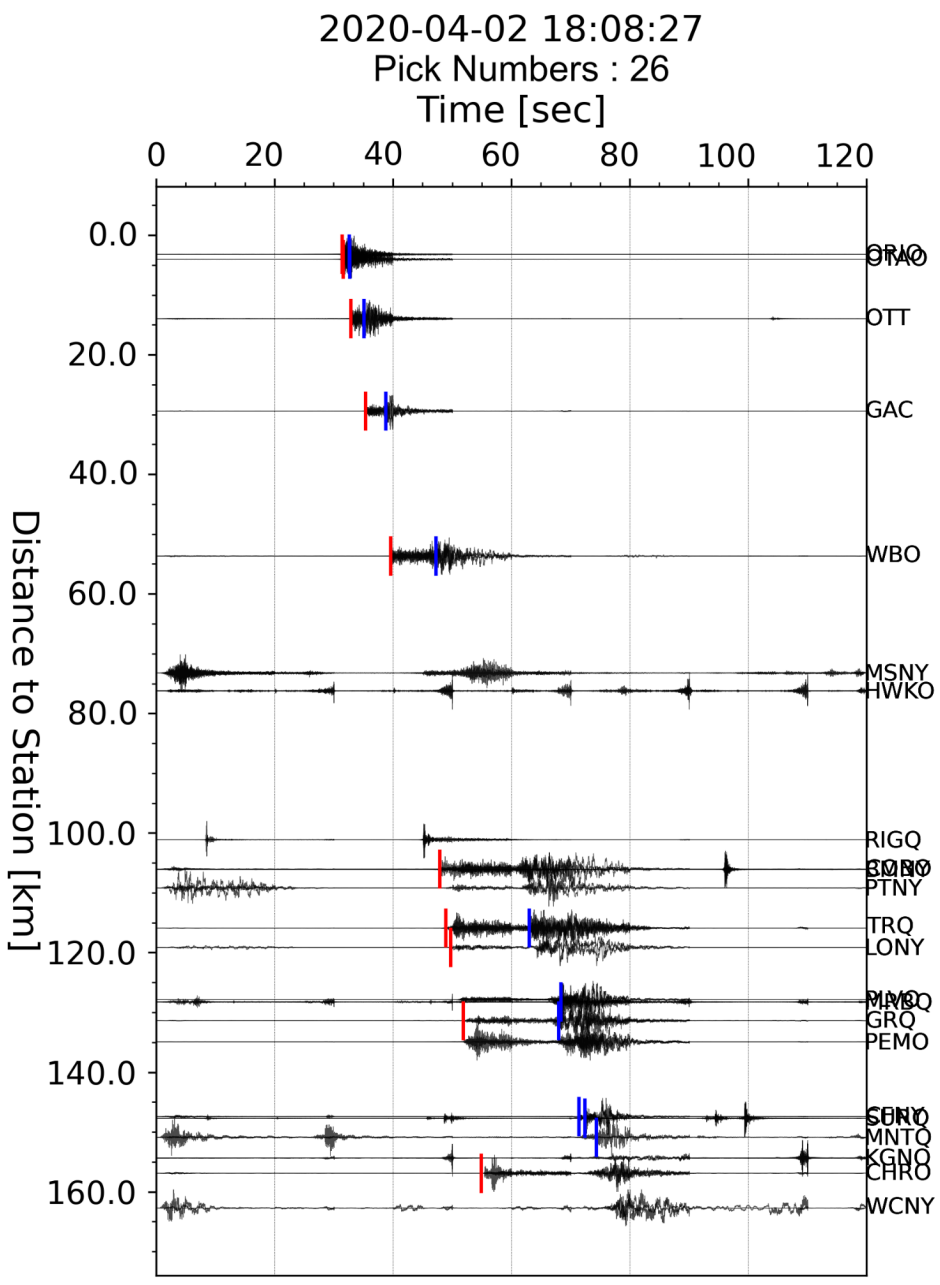

Figure S1. Example of an industrial blasting event recorded in the NEDB catalog with machine learning–based phase picking results. Red markers indicate the P phase, while blue markers indicate the S phase.

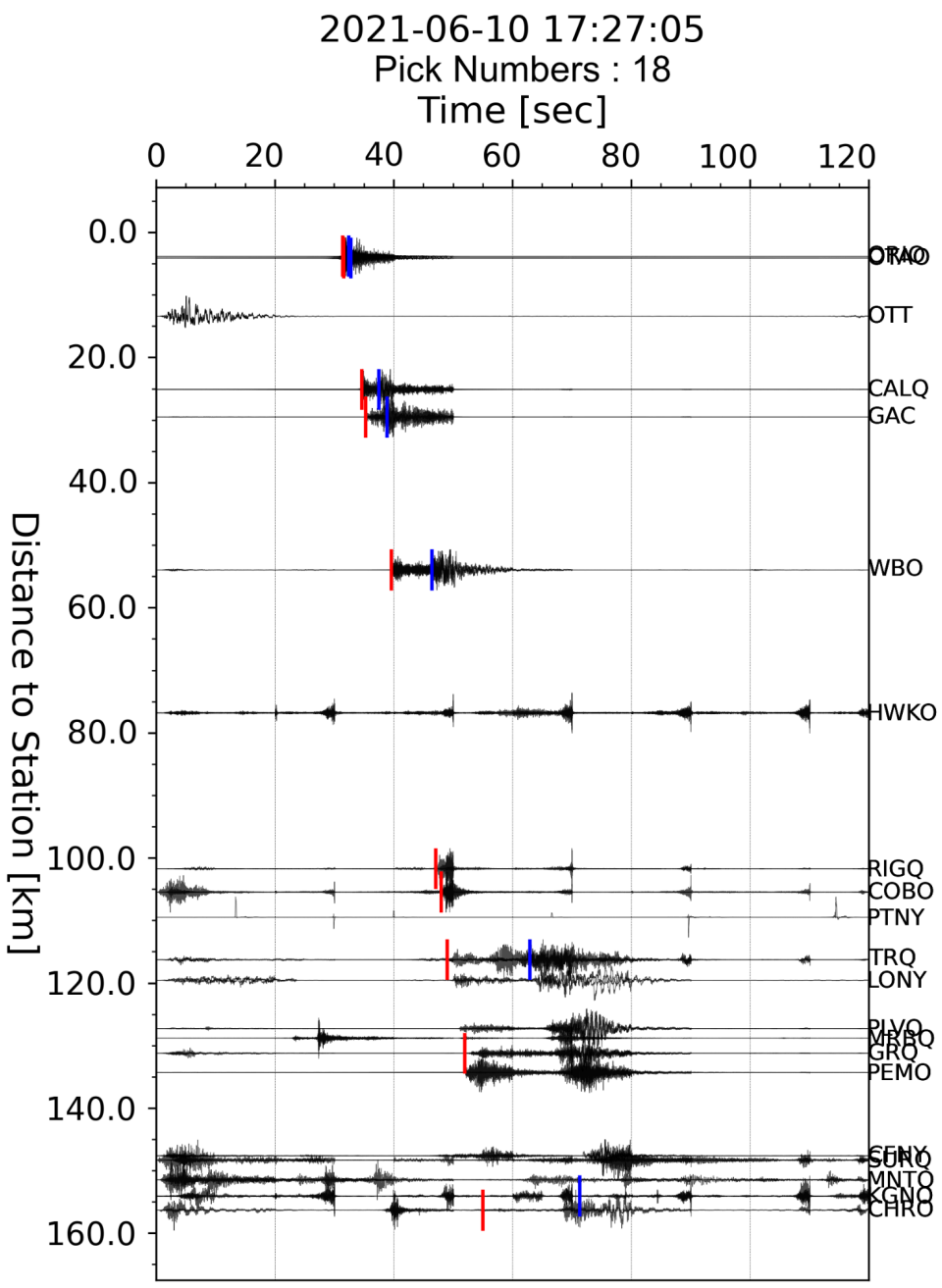

Figure S2. Example of an industrial blasting event recorded in the NEDB catalog with machine learning–based phase picking results. Red markers indicate the P phase, while blue markers indicate the S phase.

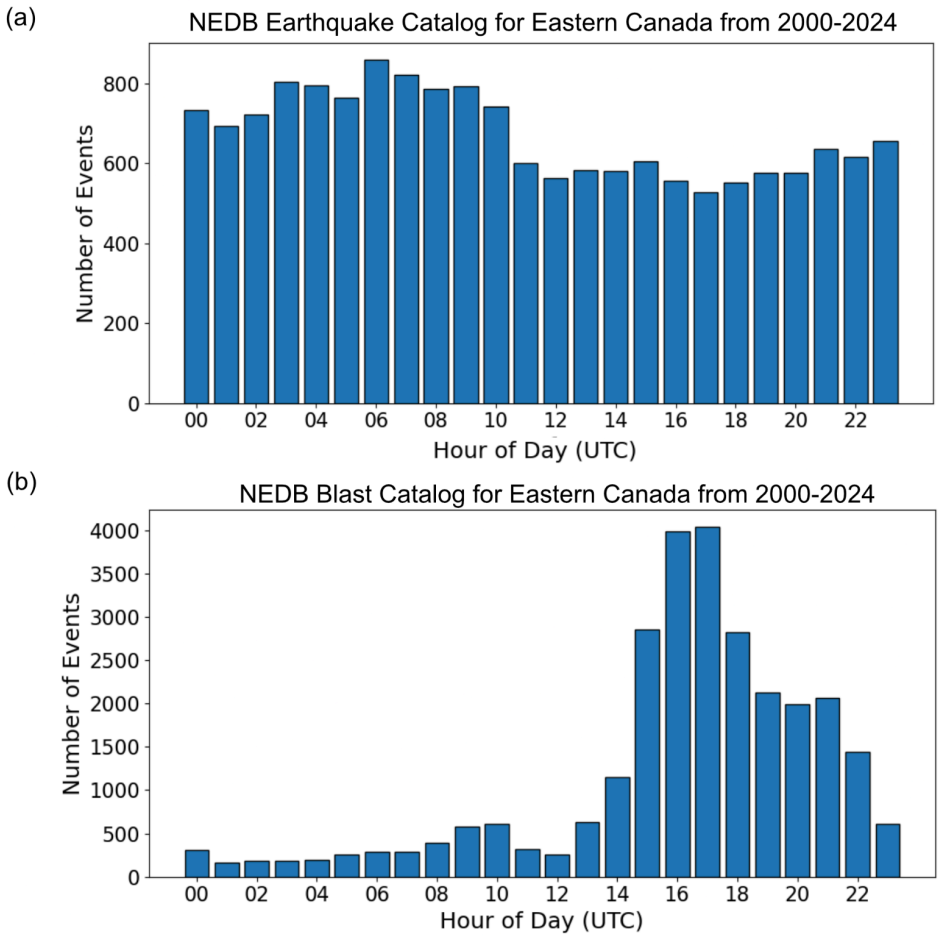

Figure S3. Hourly distribution of NEDB-cataloged (a) earthquakes and (b) industrial blast events origin times (in UTC) between 2000 and 2014 in Eastern Canada. Blasting activity is concentrated during local working hours (08:00–17:00, corresponding to UTC 12:00–21:00).

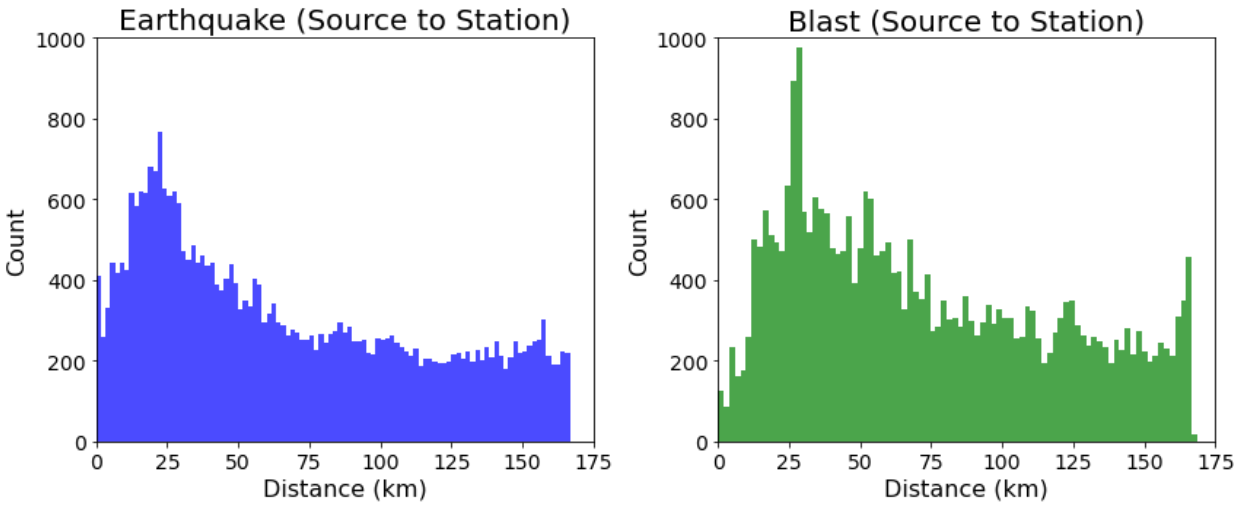

Figure S4. Histogram of source-to-station distances for all available three-component waveforms from the NEDB catalog.

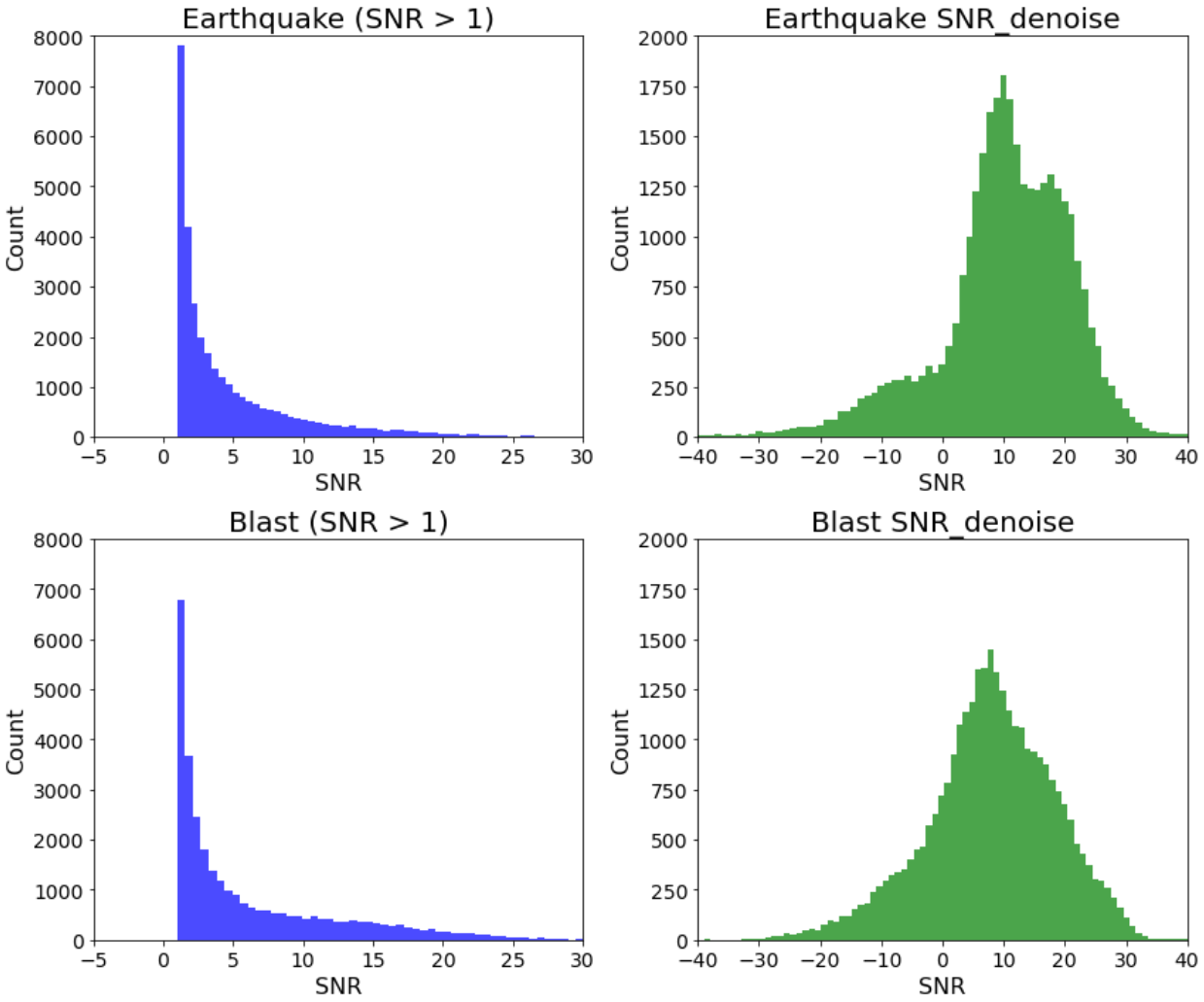

Figure S5. Comparison of the signal-to-noise ratio between the original and denoised waveforms for all cases with an original signal-to-noise ratio greater than 1.

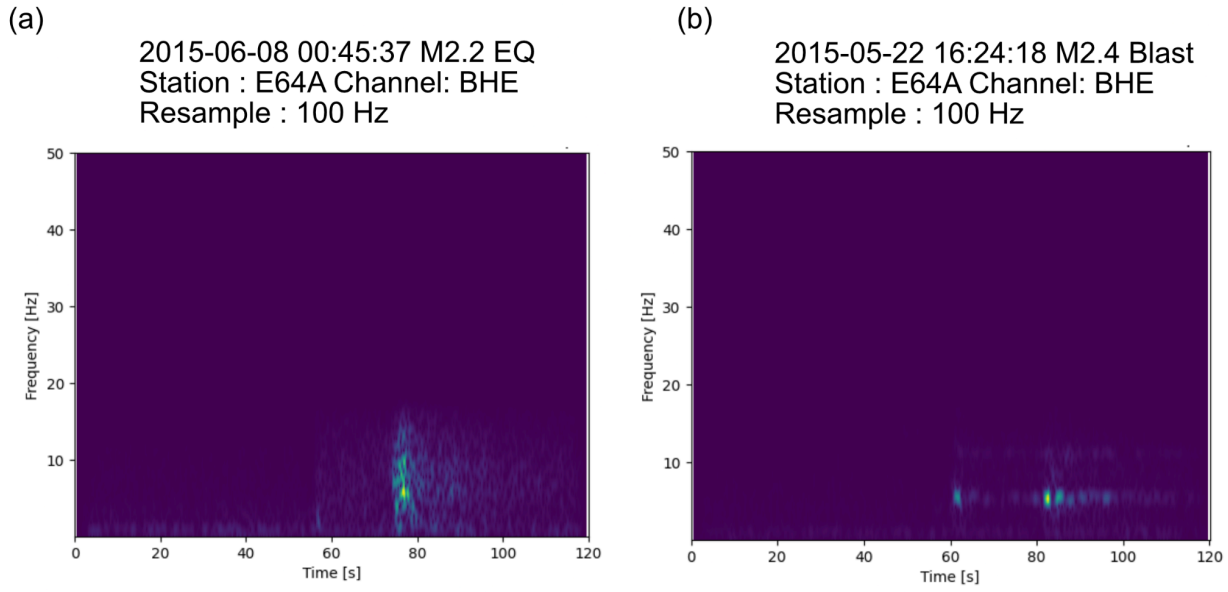

Figure S6. Spectrograms of waveforms resampled from 40~Hz to 100~Hz for (a) an earthquake and (b) a blast, corresponding to panels (b) and (e) of Figure 3 in the main text.

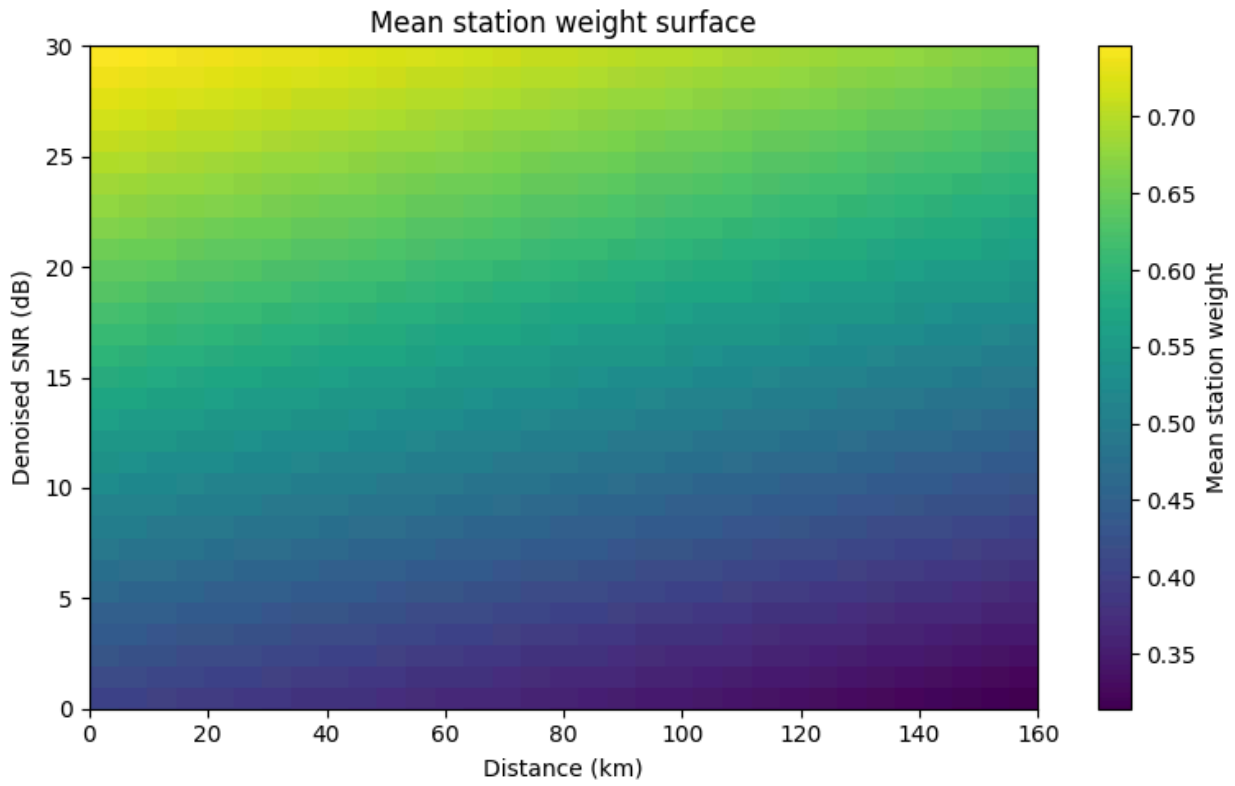

Figure S7. Reliability-based weighting for event-level classification. The weight model by logistic regression as a function of source--station distance and denoised signal to noise ratio (SNR) for 10 random seeds. For practical application, the weighting was discretized onto a regular grid with 5-km distance spacing and 1-dB SNR spacing.

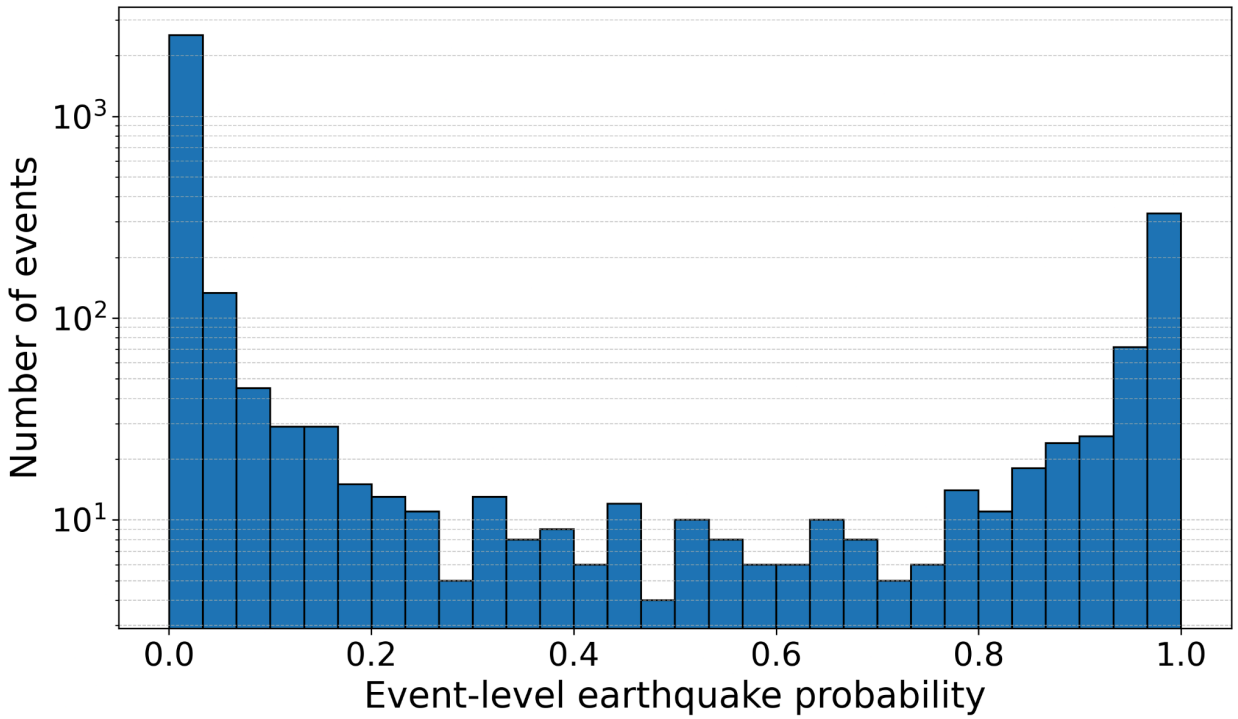

Figure S8. Distribution of prediction value of machine-learning enhanced catalog in Western Quebéc Seismic Zone from 2020 January to 2022 December.

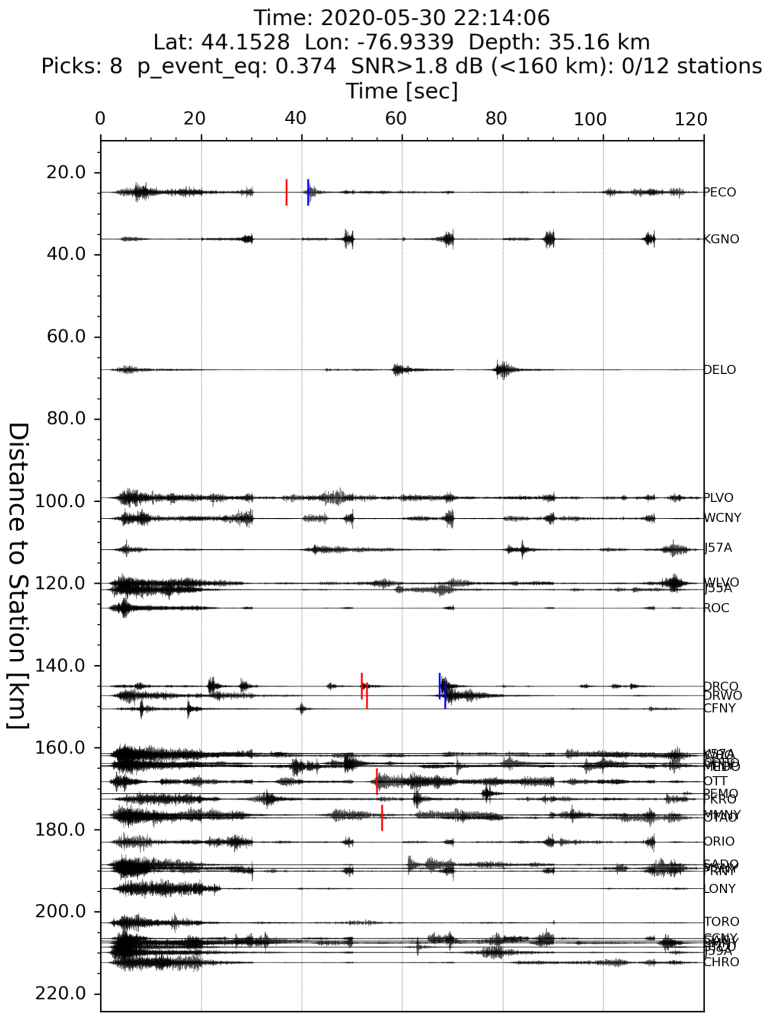

Figure S9. Example of a newly detected event that is absent from the NEDB catalog and was initially assigned a blast-like classification. Red markers indicate P-phase arrivals, whereas blue markers indicate S-phase arrivals. However, none of the station waveforms exceeds the SNR threshold, so the event is ultimately treated as a noise-dominated detection rather than a confidently classified blast. See Section 3.3 (Classification) of the main text for details on the event-level decision criteria and predicted values.

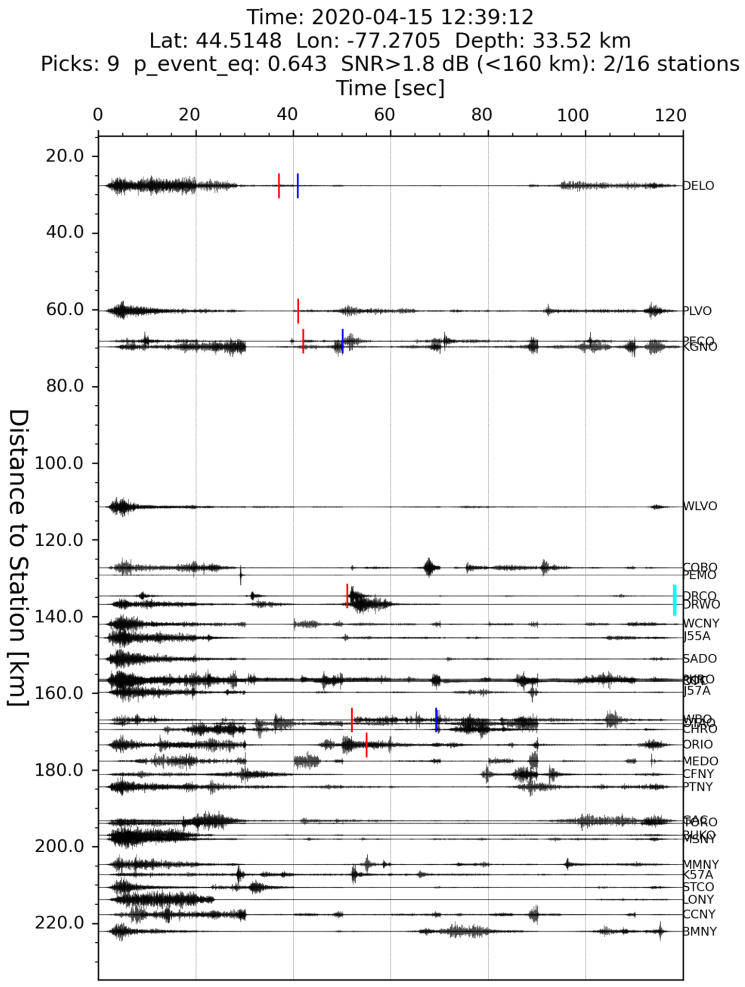

Figure S10. Example of a newly detected event that is absent from the NEDB catalog and was initially assigned an earthquake-like classification. Red markers indicate P-phase arrivals, blue markers indicate S-phase arrivals, and cyan labels denote stations whose waveforms exceed the SNR threshold. However, because fewer than three station waveforms exceed the SNR threshold, the event is ultimately treated as a noise-dominated detection rather than a confidently classified earthquake. See Section 3.3 (Classification) of the main text for details on the event-level decision criteria and predicted values.

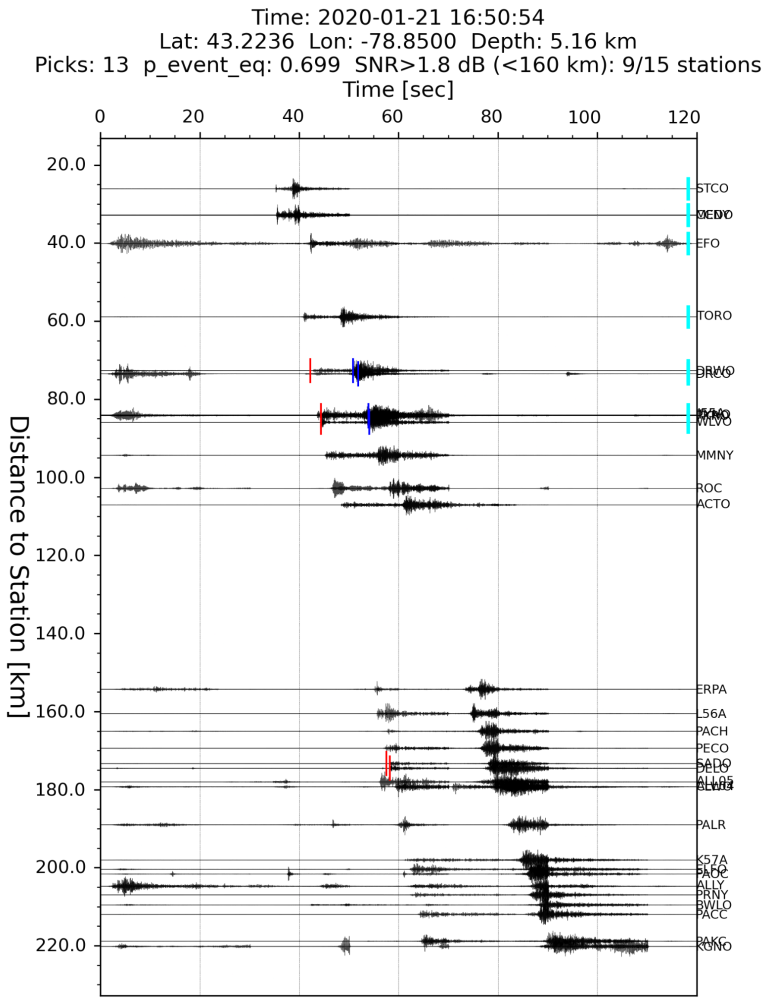

Figure S11. Example of a newly detected event that is absent from the NEDB catalog and was assigned an earthquake-like classification. Red markers indicate P-phase arrivals, blue markers indicate S-phase arrivals, and cyan labels denote stations whose waveforms exceed the SNR threshold. Because at least three station waveforms exceed the SNR threshold, the event is classified confidently as an earthquake. See Section 3.3 (Classification) of the main text for details on the event-level decision criteria and predicted values.

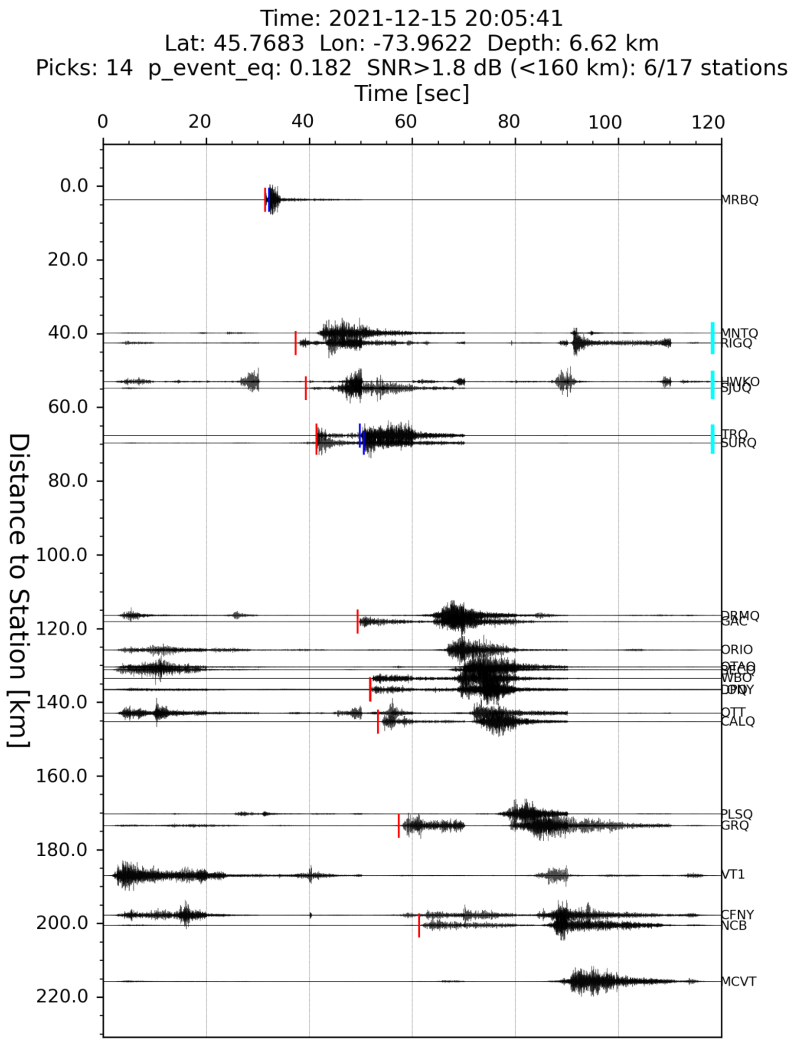

Figure S12. Example of a newly detected event that is absent from the NEDB catalog and was assigned an blast-like classification. Red markers indicate P-phase arrivals, blue markers indicate S-phase arrivals, and cyan labels denote stations whose waveforms exceed the SNR threshold. Because at least three station waveforms exceed the SNR threshold, the event is classified confidently as a blast. See Section 3.3 (Classification) of the main text for details on the event-level decision criteria and predicted values.

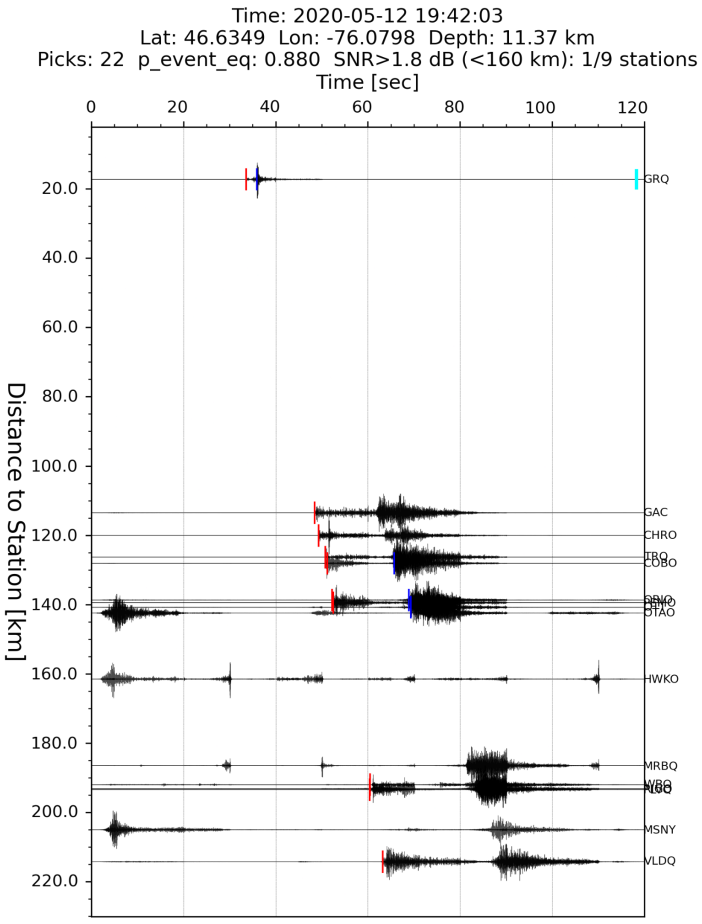

Figure S13. Example of a newly detected event that is absent from the NEDB catalog and was assigned an earthquake-like classification. Red markers indicate P-phase arrivals, blue markers indicate S-phase arrivals, and cyan labels denote stations whose waveforms exceed the SNR threshold. Because fewer than three station waveforms exceed the SNR threshold, the event would initially be treated as noise; however, because the total number of ML-picked phases exceeds 10, it is ultimately classified confidently as an earthquake. See Section~3.3 (Classification) of the main text for details on the event-level decision criteria and predicted values.

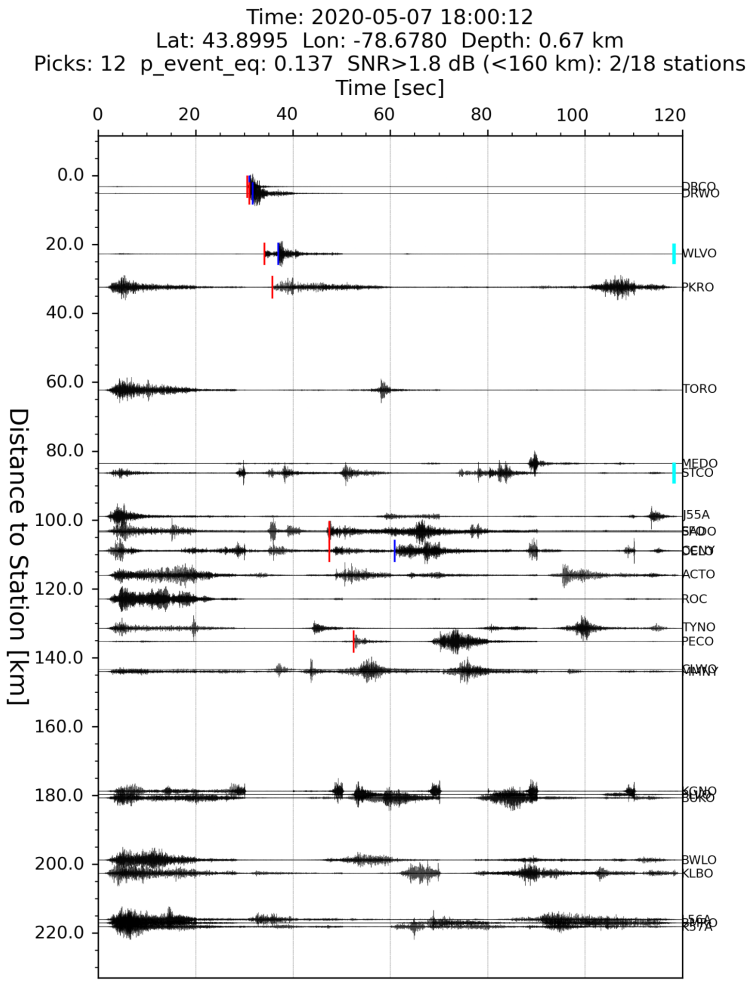

Figure S14. Example of a newly detected event that is absent from the NEDB catalog and was assigned a blast-like classification. Red markers indicate P-phase arrivals, blue markers indicate S-phase arrivals, and cyan labels denote stations whose waveforms exceed the SNR threshold. Because fewer than three station waveforms exceed the SNR threshold, the event would initially be treated as noise; however, because the total number of ML-picked phases exceeds 10, it is ultimately classified confidently as a blast. See Section~3.3 (Classification) of the main text for details on the event-level decision criteria and predicted values.

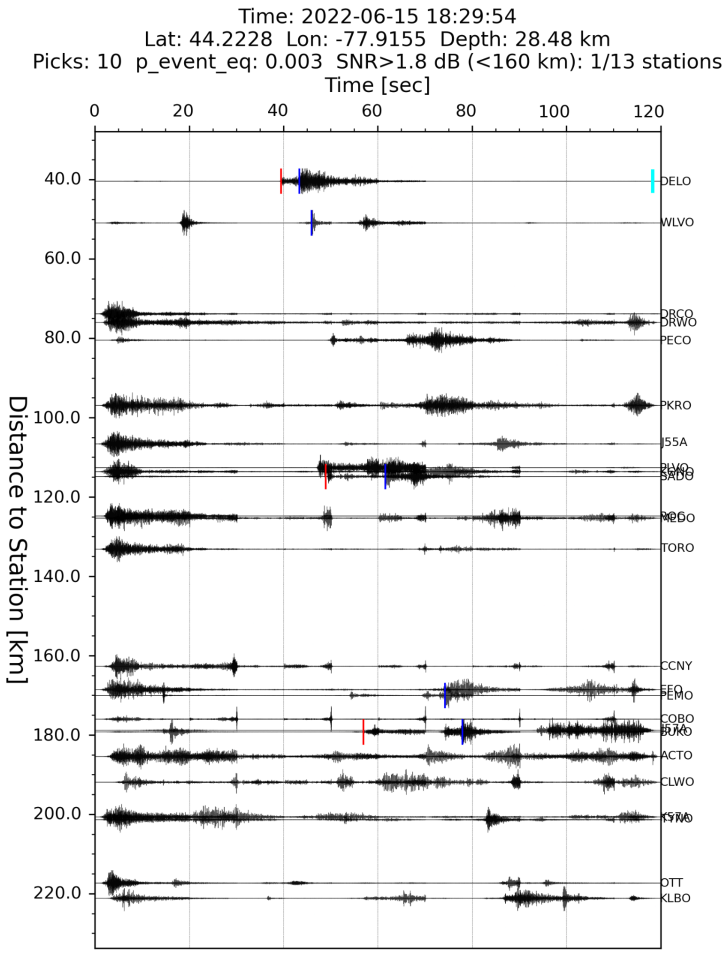

Figure S15. Example of a newly detected event that is absent from the NEDB catalog and was assigned a blast-like classification. Red markers indicate P-phase arrivals, blue markers indicate S-phase arrivals, and cyan labels denote stations whose waveforms exceed the SNR threshold. Because fewer than three station waveforms exceed the SNR threshold, the event would initially be treated as noise; however, because the event-level prediction is extreme (< 0.025), it is ultimately classified confidently as a blast. See Section~3.3 (Classification) of the main text for details on the event-level decision criteria and predicted values.

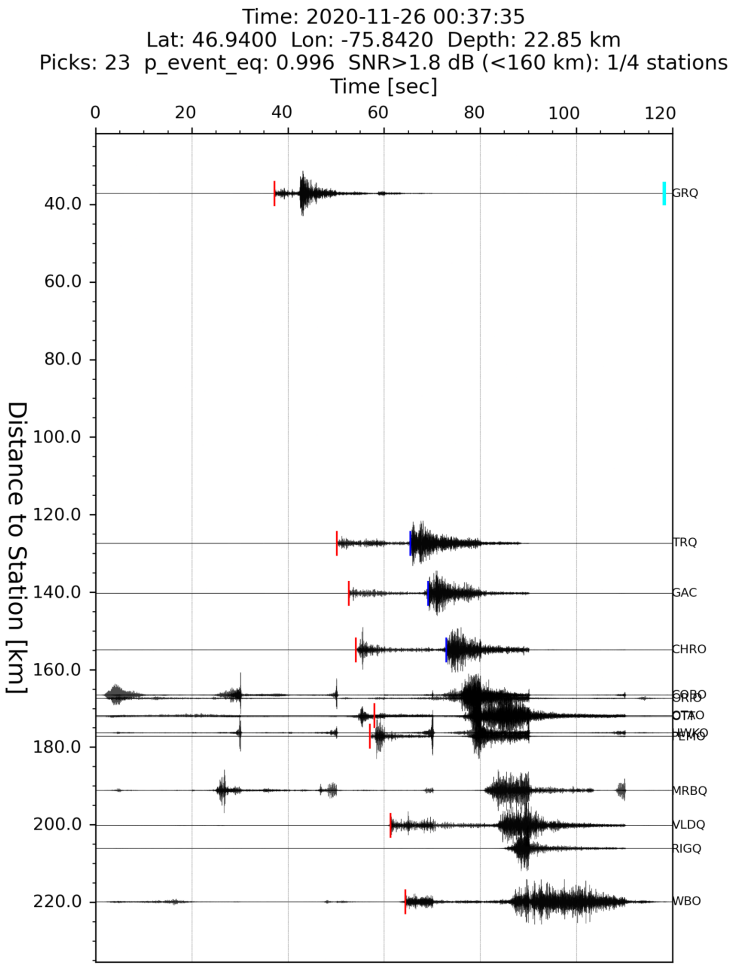

Figure S16. Example of a newly detected event that is absent from the NEDB catalog and was assigned an earthquake-like classification. Red markers indicate P-phase arrivals, blue markers indicate S-phase arrivals, and cyan labels denote stations whose waveforms exceed the SNR threshold. Because fewer than three station waveforms exceed the SNR threshold, the event would initially be treated as noise; however, because the event-level prediction is extreme (> 0.975), it is ultimately classified confidently as an earthquake. See Section~3.3 (Classification) of the main text for details on the event-level decision criteria and predicted values.

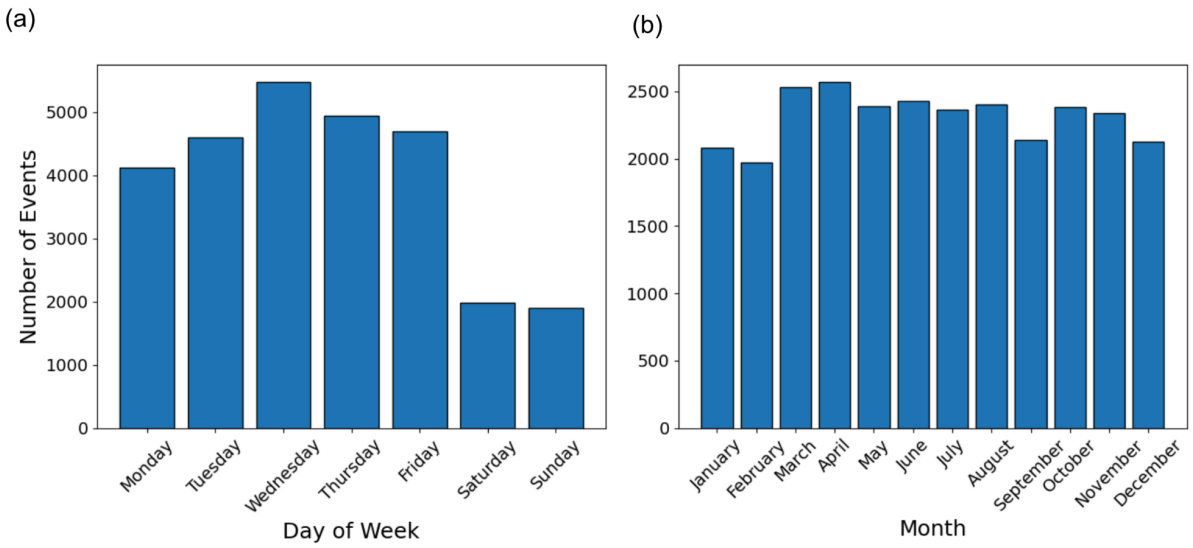

Figure S17. Histograms of industrial blasting events in Eastern Canada from the ML-enhanced catalog, aggregated by (a) day of the week (Monday through Sunday) and (b) calendar month (January through December).

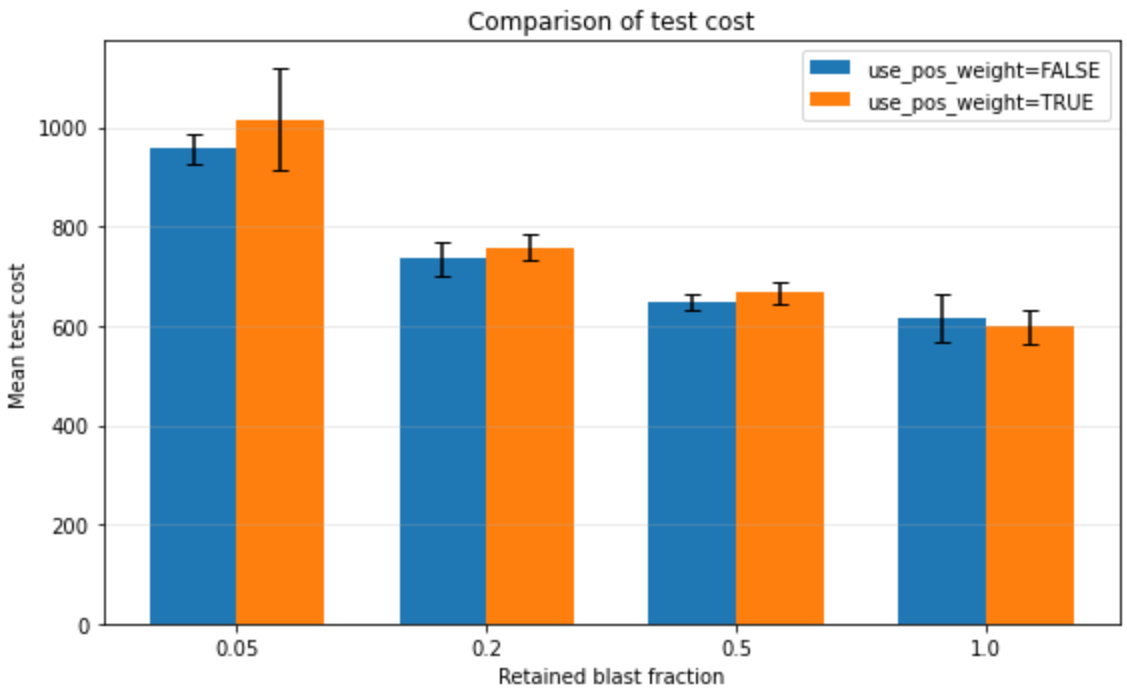

Figure S18. Comparison of mean test cost across retained blast fractions for EfficientNet+hour models trained with and without positive-class weighting. Bars show the mean test cost across random-seed experiments, and error bars indicate one standard deviation. Performance degrades markedly when the retained blast fraction falls below 0.2, whereas results for blast fractions of 0.2 and above are broadly similar. Positive-class weighting does not produce a consistent improvement in test cost.

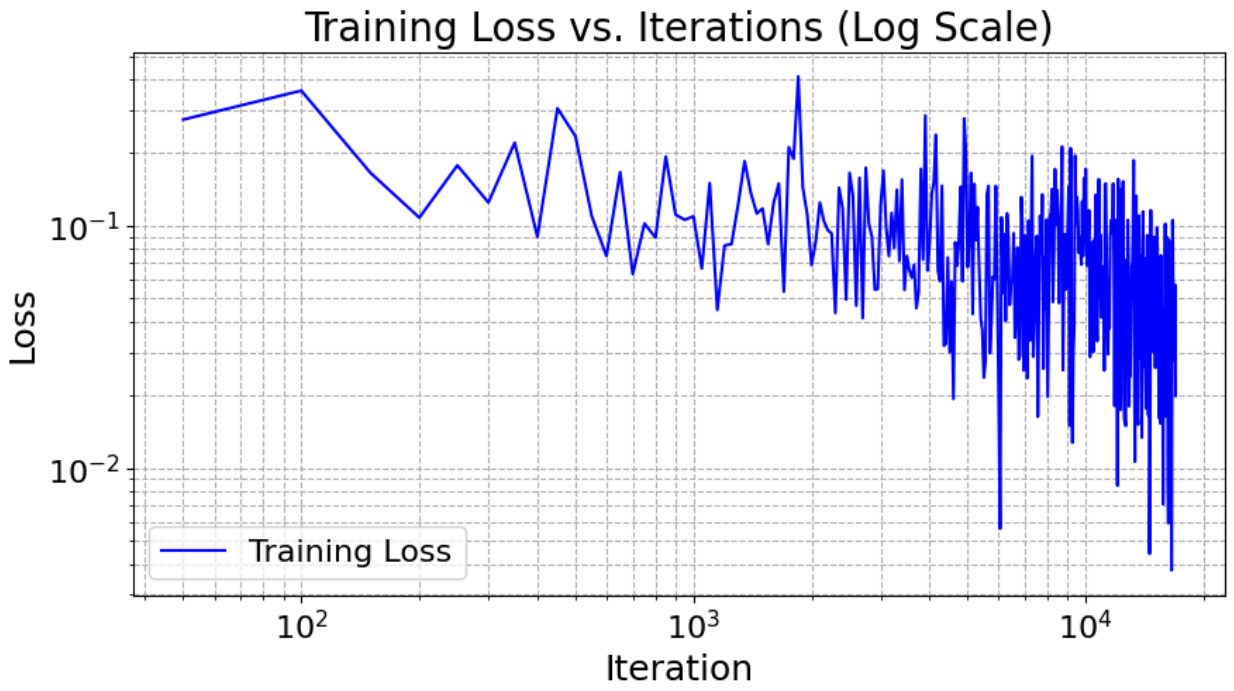

Figure S19. Temporal variation in the loss function for the final optimized EfficientNet model.

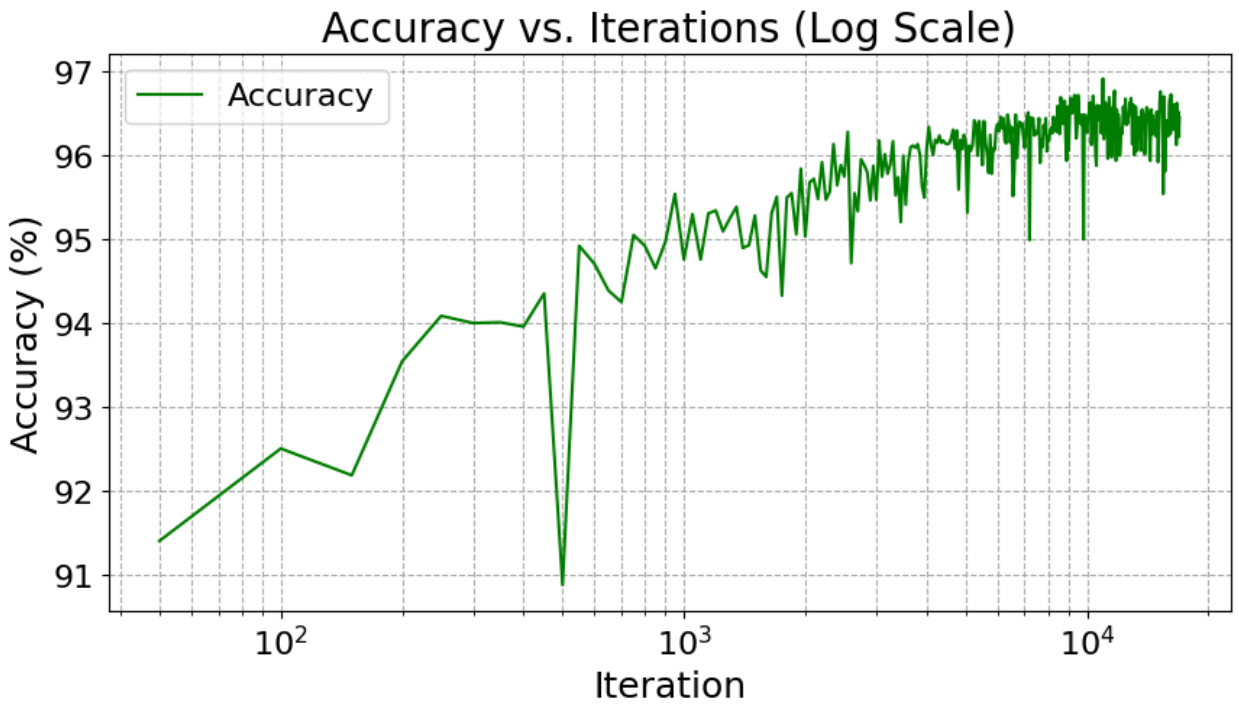

Figure S20. Temporal variation in the accuracy for the final optimized EfficientNet model.

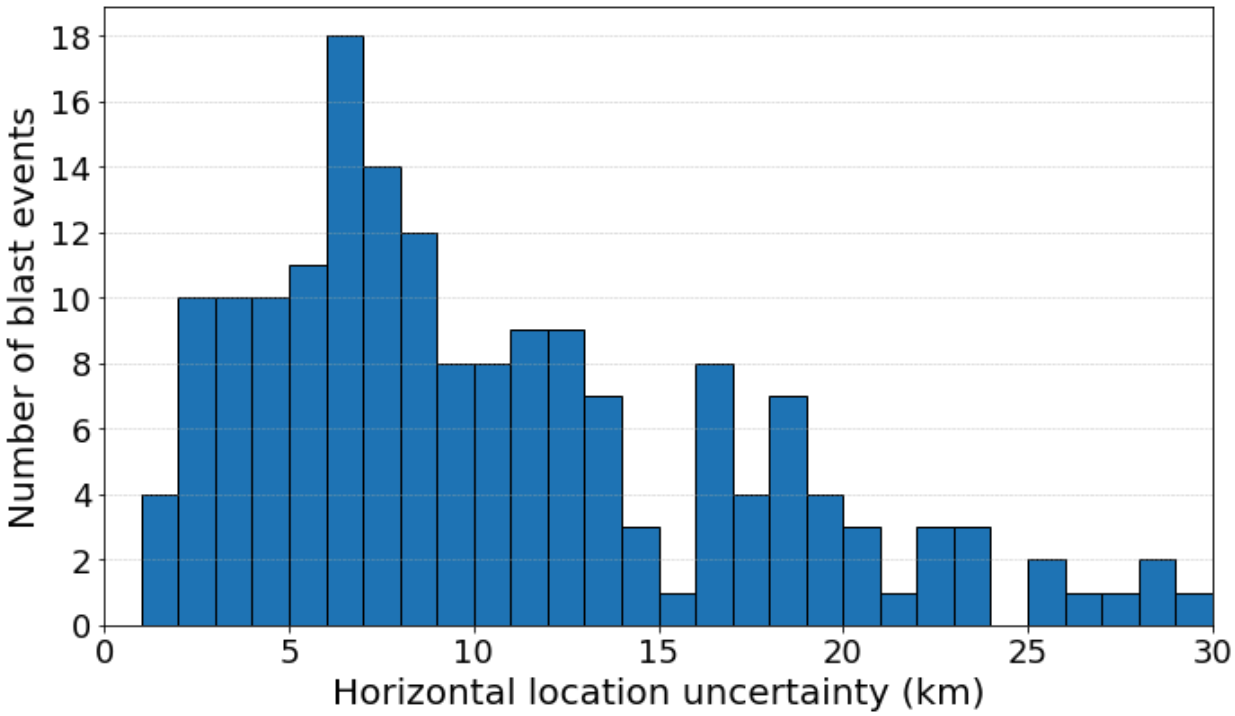

Figure S21. Horizontal location uncertainty for classified blast-like events in Charlevoix region between 2020 June to August.

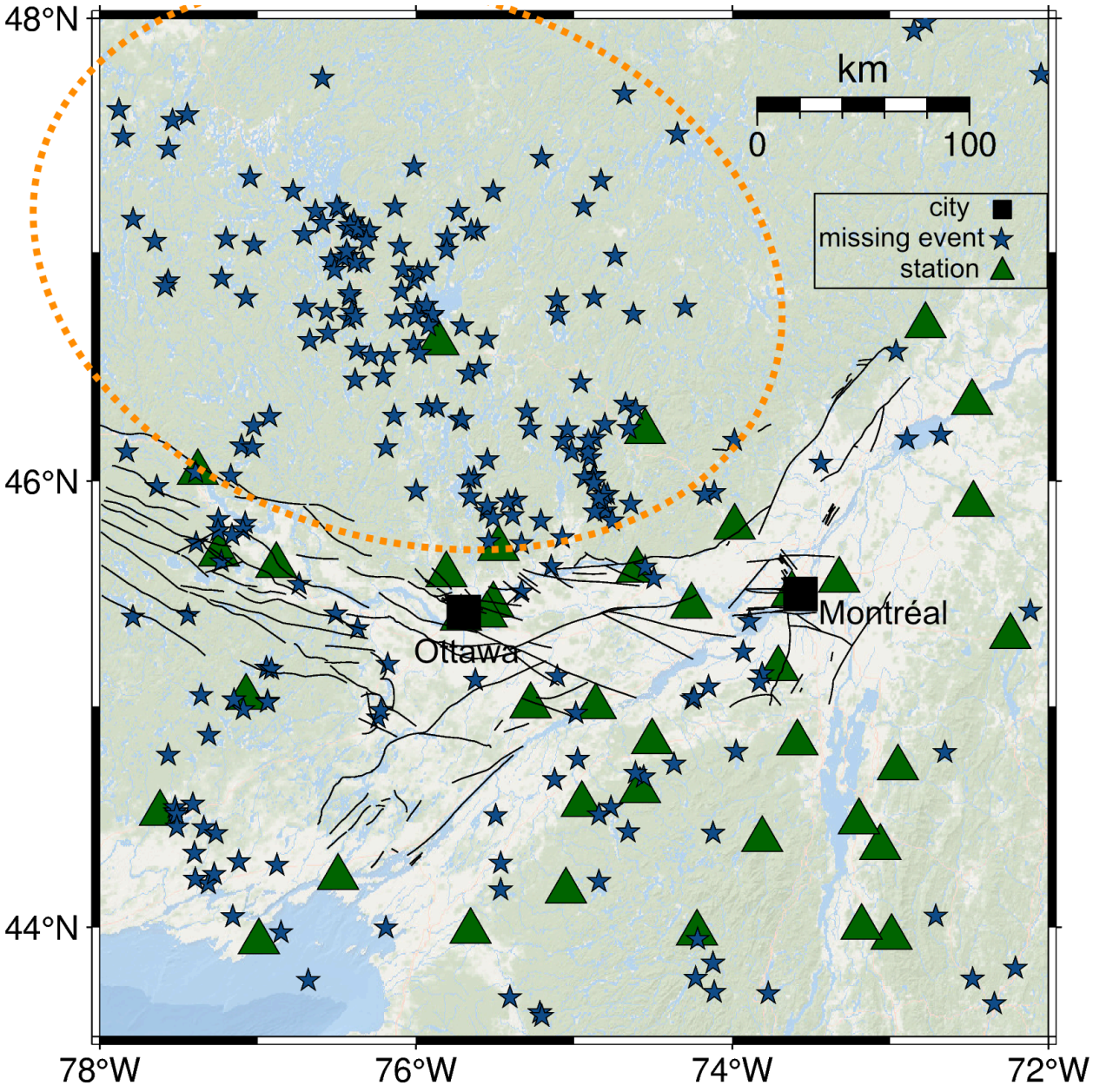

Figure S22. Distribution of pre-labeled NEDB earthquake events that were not recovered by the machine-learning catalog-enhancement algorithm in the Western Québec Seismic Zone from January 2020 to December 2022. The highlighted area indicates the region of limited seismic station coverage where most missing events are located.

Western Québec Seismic Zone	
Period	2020/01–2022/12
Earthquake in NEDB Catalog only	227
Earthquake in both catalog	224
Earthquake in ML catalog only	288
Blast in NEDB catalog only	343
Blast in both catalog	277
Blast in ML catalog only	2585

Table S1. Comparison of event catalogs between the machine-learning–enhanced catalog and the NEDB catalog for the Western Québec Seismic Zone. Events are considered identical if their epicenters lie within a 0.1° radius and their origin times differ by no more than 5s.

References

Chien, J. SABER – Spectrogram-based Algorithm for Blast and Earthquake Recognition. [Software], 2025. doi: 10.5281/zenodo.16905883.

Kao, H., Shan, S.-J., Bent, A., Woodgold, C., Rogers, G., Cassidy, J. F., & Ristau, J. (2012). Regional centroid-moment-tensor analysis for earthquakes in Canada and adjacent regions: An update. Seismological Research Letters, 83 (3), 505.

Lomax, A., Virieux, J., Volant, P., & Berge-Thierry, C. (2000). Probabilistic earthquake location in 3d and layered models: Introduction of a metropolis-gibbs method and comparison with linear locations. Advances in seismic event location, 101–134.

Mousavi, S. M., Ellsworth, W. L., Zhu, W., Chuang, L. Y., & Beroza, G. C. (2020). Earthquake transformer—an attentive deep-learning model for simultaneous earthquake detection and phase picking. Nature communications, 11 (1), 3952.

Münchmeyer, J. (2023). PyOcto: A high-throughput seismic phase associator. arXiv preprint arXiv:2310.11157.

Nuttli, O. W. (1973). Seismic wave attenuation and magnitude relations for eastern north america. Journal of Geophysical Research, 78 (5), 876–885.